Spectroscopy of ^{25}Ne and the $N = 16$ magic number

S. W. Padgett,[1] Vandana Tripathi,[1,*] S. L. Tabor,[1] P. F. Mantica,[2,3] C. R. Hoffman,[1] M. Wiedeking,[1,†] A. D. Davies,[2,4] S. N. Liddick,[2,3] W. F. Mueller,[2] A. Stolz,[2] and B. E. Tomlin[2,3]

[1]*Department of Physics, Florida State University, Tallahassee, Florida 32306, USA*

[2]*National Superconducting Cyclotron Laboratory, Michigan State University, East Lansing, Michigan 48824, USA*

[3]*Department of Chemistry, Michigan State University, East Lansing, Michigan 48824, USA*

[4]*Department of Physics and Astronomy, Michigan State University, East Lansing, Michigan 48824, USA*

(Received 12 October 2005; published 30 December 2005)

The low-energy level structure of ^{25}Ne has been investigated following the β^- decay of ^{25}F. Beta-delayed γ spectroscopy revealed new γ transitions in ^{25}Ne at 1234, 1622, and 2090 keV. The new transitions were placed in the level scheme of ^{25}Ne in accordance with the observed γ-γ coincidences. The total β^- decay strength has been accounted for. The spins and parities of the first two excited states could be ascertained by comparison with a shell model calculation and the literature. The half-life for ^{25}F decay was also remeasured using fragment-β-γ correlations, revealing a value of 90 ± 9 ms. Comparison with shell model calculations are indicative of a wider $N = 16$ gap as compared to the stable nuclei.

DOI: 10.1103/PhysRevC.72.064330 PACS number(s): 23.40.−s, 23.20.Lv, 21.60.Cs, 27.30.+t

I. INTRODUCTION

Experimental and theoretical investigations of nuclei far from stability have begun to alter some of the very basic tenets of nuclear physics. One major change has been in our understanding of magic numbers and shell gaps. It is now apparent that shell structure can vary significantly as a result of the variable contributions of nucleon-nucleon interactions and many-body dynamics, depending on Z and N. For neutron rich s-d shell nuclei, the $N = 20$ shell gap is weakened, leading to larger binding energy for ^{30,31}Na [1] and a low-lying 2^+ state in ^{32}Mg [2]. This phenomenon is related to the migration of the $0d_{3/2}$ orbital toward the fp shell [3]. This also causes an enhancement of the gap between the $1s_{1/2}$ and $0d_{3/2}$ orbitals, leading to a new magic number, $N = 16$ [4]. Several experimental observables suggest that the neutron-rich $N = 16$ isotopes for $Z = 6$–8 have a magic nature. For example, ^{22}C, ^{23}N, and ^{24}O are the last bound nuclei of their respective isotopic chains [5,6]. For doubly magic ^{24}O the predicted lowest excited state (2^+) is a $1p$-$1h$ state at 4.18 MeV, compared to the $0p$-$0h$ ground state, which is close to the neutron-decay threshold. The nonobservation of γ transitions in a recent experiment [7] confirms that $N = 16$ is magic for $Z = 8$. However, the addition of just one more proton in the $0d_{5/2}$ orbital extends the drip line for the flourine isotopes to ^{29}F, suggesting a lowering of the $0d_{3/2}$ orbital and consequent reduction of the $N = 16$ gap owing to the strong proton-neutron interaction.

The existence of the $N = 16$ shell gap for the Ne isotopes is not well understood, although it is proposed to be diminished because of the increased proton-neutron interaction from the extra proton. A single neutron removal methodology has been widely employed to study the systematics of the $d_{3/2}$ admixture in the ground state of several even-even $N = 16$ isotones for $Z \sim 10$ [8]. The assignment of $1/2^+$ to the ground state of ^{25}Ne, with negligible contribution from the $d_{3/2}$ orbital, suggests an increase in magicity or a larger gap between the $s_{1/2}$ and $d_{3/2}$ orbitals for $Z = 10$. More experimental information on the ground state and excited states for nuclei with $Z \sim 10$ and $N \sim 16$ is required to further substantiate the $N = 16$ shell gap. The correct description of low-lying excited states in nearby nuclei like ^{25}Ne is important in understanding the $N = 16$ shell gap.

Here we report the low-energy level structure of ^{25}Ne, obtained from the β^- decay of ^{25}F. Beta decay of ^{25}F has been reported earlier by Reed *et al.* [9]. Three new γ transitions from the decay of ^{25}Ne were identified in the present work. The γ-γ coincidences observed have helped to verify the placement of the new transitions in the level scheme as well as of those previously known. The β^- decay intensities were calculated and the complete β-decay strength is accounted for within error bars. The β-decay half-life of the parent nuclide, ^{25}F, was also measured from fragment-β and fragment-β-γ correlations. Exotic transfer reactions on ^{26}Mg [10,11] and a very recent (d, p) reaction with an exotic beam (^{24}Ne), [12] have also been used to study the low-lying excited states in ^{25}Ne. The present measurements complement these studies and allows for a clear comparison with the shell model calculation, suggesting a larger $N = 16$ shell gap compared to the stable nuclei.

II. EXPERIMENTAL DETAILS

The experiment was conducted at the National Superconducting Cyclotron Laboratory of Michigan State University. The nuclide of interest, ^{25}F, was produced by the projectile fragmentation of a 140 MeV/nucleon ^{48}Ca^{20+} beam (10–15 particle-nA) on a Be target of thickness 733 mg/cm^2 placed at the object position of the A1900 fragment separator. A 300 mg/cm^2 wedge-shaped Al degrader was used at the intermediate image position of the A1900 for separating the

*Corresponding author

†Present address: Lawrence Berkeley National Laboratory, Berkeley, California 94720, USA.

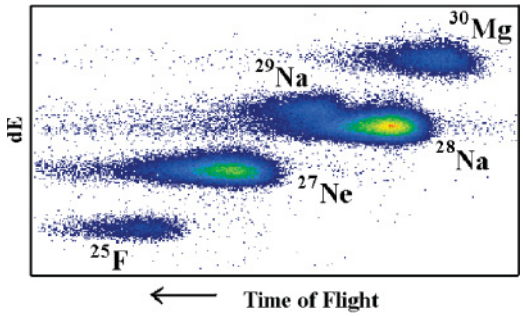

FIG. 1. (Color online) Time of flight vs *dE* particle identification plot used to differentiate the different nuclides reaching the DSSD.

ions according to their M/Z ratios. The A1900 magnetic fields were set to 4.35 and 4.21 Tm with a 1% momentum acceptance. With these settings a "cocktail" secondary beam consisting of F, Ne, Na, and Mg isotopes was obtained. These exotic nuclides were transported to the Beta Counting Station (BCS) [13] and implanted in the DSSD (double-sided Si microstrip detector), part of the BCS. A 10-mm Al degrader was placed in front of the DSSD to ensure complete implantation within the 985-μm-thick DSSD. Energy loss and time-of-flight information were used to differentiate the different species reaching the DSSD. A plot of time of flight versus *dE* is shown in Fig. 1, where the various species reaching the DSSD are cleanly separated. Each implantation event was recorded and tagged with an absolute time stamp generated by a free-running clock (30.5-μs repetition rate).

Fragment-β correlations were established in software, where a low-energy β event was correlated with a high-energy implant event in the same or adjacent pixels of the DSSD. Light particles, transmitted along with the secondary beam, were vetoed by a scintillator placed at the end of the BCS for the purpose of increasing the fragment-β correlation efficiency. To generate a decay curve, the differences between the absolute time stamps of the correlated β and implant events were histogrammed. Implant events were rejected if not followed by a β event within a certain time period in the same or an adjacent pixel or if a second implantation occurred before a β decay. This was helpful in suppressing background. A 500-ms time period was chosen for analyzing the β-delayed γ transitions from ^{25}F, whereas a 5-s time period was selected to generate the decay curve. The β-delayed γ rays were detected using 12 detectors of the Segmented Germanium Array (SeGA) [14] arranged around the BCS. The efficiency of the SeGA was measured to be ~5% at 1 MeV. Further details of the experimental and electronic setup can be found in Ref. [15].

III. RESULTS

A. Half-life measurement

The decay curve for ^{25}F, derived from β-decay correlated implants, is shown in Fig. 2 for events collected for 5 s after the initial implantation. By using the Bateman equations for radioactive decay series, a three-component exponential fit was made to the decay curve. This accounted for the decay

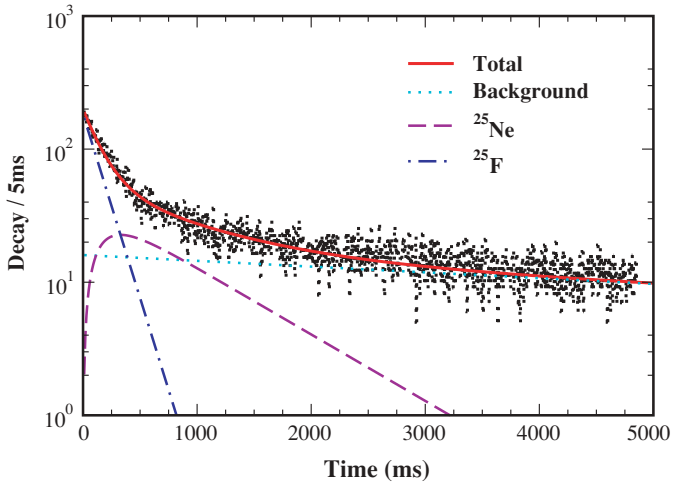

FIG. 2. (Color online) The decay curve for ^{25}F. Shown are the total fit to the decay curve, which includes the parent decay, daughter growth and decay, and the background along with the individual components. The half-life obtained for the decay of ^{25}F is 112 ± 5 ms.

of ^{25}F, the growth and decay of the daughter nucleus ^{25}Ne, and the background. Since the half-life of ^{25}Ne is known with good accuracy from previous work, it was kept fixed at 602 ± 8 ms [16] during the fitting. A slow exponentially falling background was adjusted to account for the long-lived contaminants. The individual components and the total fit are shown in Fig. 2. A half-life of 112 ± 5 ms was obtained from the present work. Previous measurements of the half-life of ^{25}F are 50 ± 6 ms [9], 59 ± 40 ms [17], and 70 ± 10 ms [18]. Hence, our result suggests a longer half-life for the decay of ^{25}F than reported before. Since the decay curve from fragment-β correlations could suffer from an inaccurate estimation of the long-lived background, an additional constraint of a γ transition in ^{25}Ne was used to generate decay curves, shown in Fig. 3, these are also consistent with a longer half-life for the decay of ^{25}F. We consider these values (89 ± 12 and 91 ± 13 ms) more reliable and an average of the two values from Fig. 3 was used to calculate the log *ft* values. The fit to the decay curve was also used to estimate the initial number of β-decaying particles implanted into the DSSD, which was about 5500. This initial activity is required to calculate the absolute β-decay intensities to each level of ^{25}Ne populated by the decay of ^{25}F.

B. Level scheme

The β-delayed γ spectrum observed within 500 ms from the initial ^{25}F implant is shown in Fig. 4. The spectrum displays γ lines representing transitions in ^{25}Ne following the β^- decay of ^{25}F. The 1702-, 1613-, 2186-, and 574-keV γ transitions have been reported previously for ^{25}Ne [9]. Three new γ transitions of 1622, 2090, and 1234 keV were observed for the first time in the present study. Decay curves in coincidence with these γ transitions yielded consistent half-lives, justifying their place in the level scheme of ^{25}Ne. The strong 90-keV γ transition is from the granddaughter nucleus, ^{25}Na, whereas the 1982-keV line is from ^{24}Ne resulting from the β-n decay of ^{25}F.

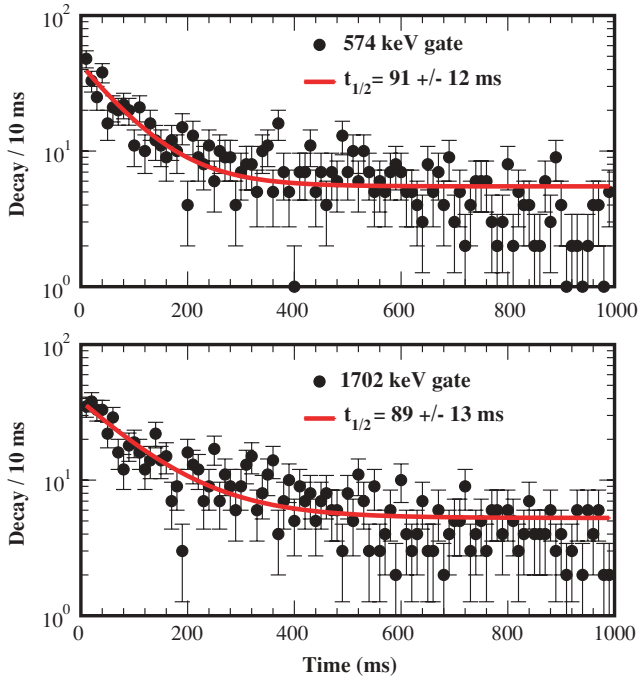

FIG. 3. (Color online) The decay curve for ^{25}F in coincidence with the 574- and the 1702-keV transitions in ^{25}Ne. A constant background was assumed in both cases.

The 2236-keV transition was identified as arising from a contaminant entering the DSSD, because of its longer half-life.

The fragment-β-γ-γ coincidences observed are displayed in Fig. 5. Coincidences are observed among the 574-, the 1613-, and the 1702-keV γ transitions (Fig. 4). This cascade

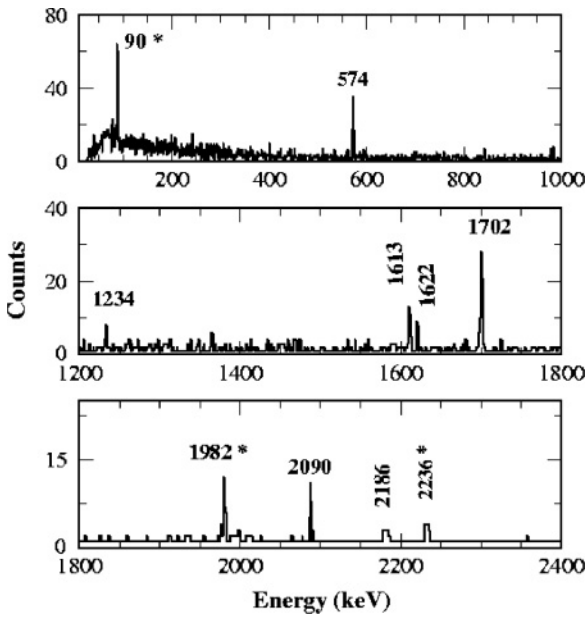

FIG. 4. β-delayed γ spectrum from events coming within 500 ms of a ^{25}F implant. Gamma transitions from ^{25}Ne are shown, including the new transitions at 1234, 1622, and 2090 keV. The 90-keV γ transition is from ^{25}Na; the 1982-keV one is from ^{24}Ne formed by β-n decay.

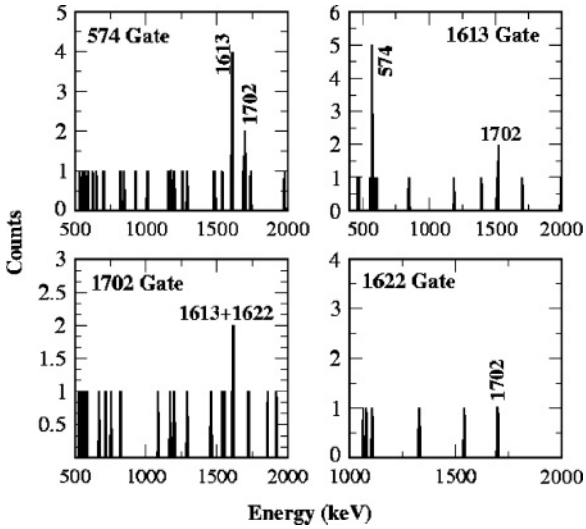

FIG. 5. The fragment-β-γ-γ coincidences observed from gating on γ transitions in ^{25}Ne.

of γ transitions generates two excited states at 1702 and 3315 keV, confirming the placement of these transitions in Ref. [9]. Coincidences between the 1622- and 1702-keV transitions (Fig. 4) establish a new level at 3324 keV. The energies of the other new transitions observed, 2090 and 1234 keV, suggest that these γ transitions form a different decay path for the 3324-keV state. Based on the observed coincidences and the energy and intensity sum rules, the proposed level scheme for ^{25}Ne is shown in Fig. 6. Previously a tentative level at 4092 keV was placed in the level scheme of ^{25}Ne [9], decaying

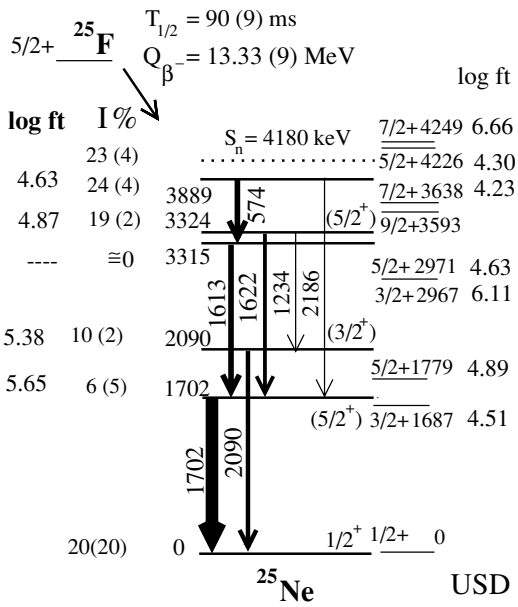

FIG. 6. Proposed level scheme for ^{25}Ne obtained from the β^- decay of ^{25}F to the various energy levels in ^{25}Ne. The β-decay branchings are shown with the log ft values for each level on the left; the USD shell model calculations are shown on the right. The tentative spin and parity assignments to the excited states are also indicated.

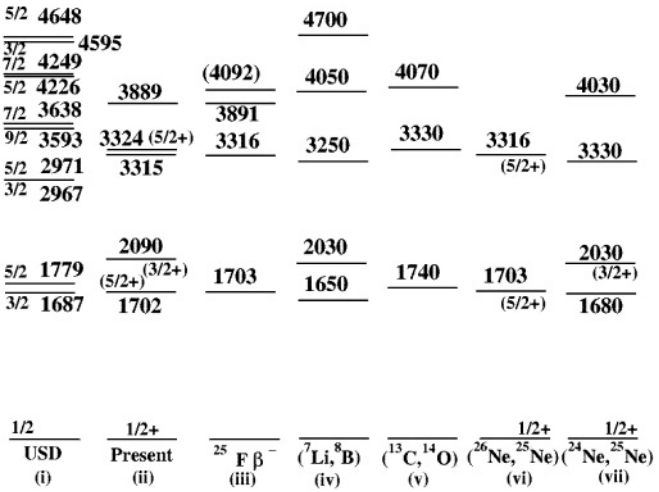

FIG. 7. Comparison of (i) ^{25}Ne levels from the USD shell model [19] (all states have positive parity), (ii) level scheme from the present work, (iii) partial level scheme from the previous β-decay study [9], and energy levels identified in transfer reactions: (iv) (^{7}Li,^{8}F) [10], (v) (^{13}C,^{14}O) [11], (vi) one-neutron knockout from ^{26}Ne [8], and (vii) one-neutron pickup ^{24}Ne(d, p)^{25} [12].

by a very weak γ transition of 776 keV to the proposed 3316-keV level (see Fig. 7). However, the 776-keV γ transition was not observed in this experiment and hence not placed in the level scheme.

The absolute β-decay branching to each populated level was calculated from the differences between γ-ray intensities feeding into and out of that level, using the measured SeGA efficiency and utilizing the initial number of β-correlated decay events obtained from a fit to the decay curve. The large Q_β window (13.33 $\pm$ 0.09 MeV) [20] for ^{25}F and small neutron separation energy ($\sim$4.2 MeV) in the daughter nucleus, ^{25}Ne, also allows for the population of neutron unbound states after β decay. The neutron unbound states decay by neutron emission to excited (or ground) states in daughter nuclei. The probability of one-neutron emission after β decay, P_n, estimated from the γ activity of the daughter nucleus, ^{24}Ne, is 23.1 $\pm$ 4.5%. The values reported in the literature for P_n are 14 $\pm$ 5% [9] and 15 $\pm$ 10% [17] obtained using neutron detectors. The log *ft* values were calculated for the bound levels in ^{25}Ne according to Ref. [21] using the measured absolute intensities for βdecay, the measured half-life, and the Q_β values from the literature [20].

IV. DISCUSSION

The proposed level scheme for ^{25}Ne has been compared with *s*-*d* shell model predictions using the USD (Universal SD) interaction [19] and previous work (Figs. 6 and 7). A firm $1/2^+$ spin-parity assignment has been made for the ground state of ^{25}Ne [8], which agrees with extreme single-particle shell model predictions. The absence of a large β-decay branch to the ground state is consistent with this assignment. The ground-state spin of ^{25}F has been measured to be $5/2^+$ from a one-neutron removal reaction [22]. A tentative spin assignment of $5/2^+$ was made to the excited state at 1703 keV by Terry *et al*. [8] after comparing the extracted momentum distribution for these excited states with an Eikonal model. Shell model calculations for ^{25}Ne using the USD interaction predict two levels close to 1.7 MeV excitation energy with spins $3/2^+$ and $5/2^+$, of which the $3/2^+$ level is predicted to have a larger β-decay branch. Comparison of these log *ft* values with the present work suggests that the first excited level observed at 1702 keV represents the $5/2^+$ level, consistent with the tentative spin assignment from Ref. [8]. This means that the 2090-keV state is the first $3/2^+$ exited state. This bridges the results of the neutron pickup on ^{24}Ne [12] with the neutron knockout reaction. In the ^{24}Ne(d, p)^{25}Ne reaction studied by Catford *et al*. [12], the level at 2.03 MeV is populated much more strongly than the level seen at 1.68 MeV, and hence it was associated with the $J^\pi = 3/2^+$ state, by considering the larger spectroscopic factor for a $J^\pi = 3/2^+$ state. Keeping in mind the better energy resolution of the present experiment, we conclude that the 2.03-MeV level of Ref. [12] must be the 2090-keV state observed in the present work and the 1.68-MeV level must correspond to the 1702-keV state. Thus the present study clearly resolves the spin assignments for the first two excited states in ^{25}Ne, which happen to be reversed as compared to the shell model predictions.

In the knockout reaction, a tentative assignment of $5/2^+$ was also made to the level at 3315 keV. This is inconsistent with the present work, as this state has negligible direct β feeding. Given that the ground state of ^{25}F is $5/2^+$, population of this state is allowed by spin selection rules. In the present study we observe a doublet of states at $\sim$3.3 MeV, not seen in the previous β-decay study [9]. In an earlier exotic transfer measurement by C. L. Woods *et al*. [11], ^{26}Mg(^{13}C,^{14}O)^{25}Ne, it was also proposed that the level at 3.33 MeV has two unresolved components. A likely possibility is that the state observed in the knockout reaction, given the limited energy resolution, is the near-by state at 3324 keV, which agrees with the $5/2^+$ shell model state at $\sim$2.9 MeV with large β-decay branching. This leaves two choices for the 3315-keV state: (i) It could correspond to the $3/2^+$ shell model state at $\sim$2.9 MeV with small β-decay branching, or (ii) it could be the $9/2^+$ shell model state at $\sim$3.59 MeV. In the first scenario, the 3889-keV state would most likely be the $5/2^+$ state at $\sim$4.2 MeV, in the second, it could be the $7/2^+$ state at $\sim$3.6 MeV, since the 574-keV transition should be an $M1$ transition given its decay properties.

Though the shell model agrees reasonably with the experimentally observed states, there are some noticeable discrepancies. Most prominently, the proposed $3/2^+_1$ state at 2090 keV is about 400 keV higher than the shell model state at 1687 keV. Also, it is higher than the $5/2^+_1$ state as opposed to the shell model calculations. This trend is correctly reproduced by a very recent calculations by Brown [23] using a new USD interaction USD-05 that has an expanded experimental data base, especially for nuclei with large isospin. This suggests that the energy of the $d_{3/2}$ neutron orbital rises in $N = 15$ isotones when protons are removed from the $d_{5/2}$ orbital, causing an enhanced gap between the $1s_{1/2}$ and $0d_{3/2}$ orbitals and leading to the $N = 16$ shell gap for $Z \sim 10$. Support for this observation can also be found by looking at the level structure of ^{27}Mg; here one finds the lowering of the $d_{3/2}$

orbital with the addition of just two extra protons. The first excited state of ^{27}Mg is a $3/2^+$ state at 985 keV, compared to 2090 keV for ^{25}Ne. Also, the ground state of ^{27}Mg is found to have a much larger admixture of the $3/2$ orbital compared to ^{25}Ne [8]. This seems to suggest that for a more neutron rich isotone like ^{25}Ne the $0d_{3/2}$ orbital moves closer to the *fp* shell, increasing the $N = 16$ shell gap. However, detailed shell model calculations are required to ascertain whether the differences seen between the experimental and shell model energies are related to the $N = 16$ shell gap.

V. SUMMARY

In summary, we investigated the low-energy level structure of ^{25}Ne populated in the β decay of ^{25}F. Two new levels and three new transitions could be identified in the present work. Placement of the observed transitions was confirmed by fragment-β-γ-γ coincidences. Comparisons with USD shell model calculations show a reasonable agreement with the experimental level scheme. The spin and parities of the first two excited states could be fixed by comparison with shell model predictions and previous work. A clear offset is observed, with the $3/2^+_1$ experimental level lying higher than those predicted by the shell model. This may suggest a larger $N = 16$ shell gap than that assumed in the USD interaction.

ACKNOWLEDGMENTS

This work was supported by NSF Grant Nos. PHY-01-39950 and PHY-01-10253. The authors thank the NSCL operations staff for the smooth conduct of the experiment.

[1] C. Thibault, R. Klapisch, C. Rigaud, A. M. Poskanzer, R. Prieels, L. Lessard, and W. Reisdorf, Phys. Rev. C **12**, 644 (1975).
[2] T. Motobayashi, Y. Ikeda, Y. Ando, K. Ieki, M. Inoue, N. Iwasa, T. Kikuchi, M. Kurokawa, S. Moriya, S. Ogawa, H. Murakami, S. Shimoura, Y. Yanagisawa, T. Nakamura, Y. Watanabe, M. Ishihara, T. Teranishi, H. Okuno, and R. F. Casten, Phys. Lett. **B346**, 9 (1995).
[3] T. Otsuka, R. Fujimoto, Y. Utsuno, B. A. Brown, M. Honma, and T. Mizusaki, Phys. Rev. Lett. **87**, 082502 (2001).
[4] A. Ozawa, T. Kobayashi, T. Suzuki, K. Yoshida1, and I. Tanihata, Phys. Rev. Lett. **84**, 5493 (2000).
[5] O. Tarasov, R. Allatt, J. C. Angelique, R. Anne, C. Borcea, Z. Dlouhy, C. Donzaud, S. Grevy, D. Guillemaud-Mueller, M. Lewitowicz, S. Lukyanov, A. C. Mueller, F. Nowacki, Yu. Oganessian, N. A. Orr, A. N. Ostrowski, R. D. Page, Yu. Penionzhkevich, F. Pougheon, A. Reed, M. G. Saint-Laurent, W. Schwab, E. Sokol, O. Sorlin, W. Trinder, and J. S. Winfield Phys. Lett. **B409**, 64 (1997).
[6] H. Sakurai, S. M. Lukyanov, M. Notani, N. Aoi, D. Beaumel, N. Fukuda, M. Hirai, E. Ideguchi, N. Imai, M. Ishihara, H. Iwasaki, T. Kubo, K. Kusaka, H. Kumagai, T. Nakamura, H. Ogawa, Yu. E. Penionzhkevich, T. Teranishi, Y. X. Watanabe, K. Yoneda, and A. Yoshida, Phys. Lett. **B448**, 180 (1999).
[7] M. Stanoiu, F. Azaiez, Z. Dombradi, O. Sorlin, B. A. Brown, M. Belleguic, D. Sohler, M. G. Saint Laurent, M. J. Lopez-Jimenez, Y. E. Penionzhkevich, G. Sletten, N. L. Achouri, J. C. Anglique, F. Becker, C. Borcea, C. Bourgeois, A. Bracco, J. M. Daugas, Z. Dlouhy, C. Donzaud, J. Duprat, Z. Fulop, D. Guillemaud-Mueller, S. Grevy, F. Ibrahim, A. Kerek, A. Krasznahorkay, M. Lewitowicz, S. Leenhardt, S. Lukyanov, P. Mayet, S. Mandal, H. van der Marel, W. Mittig, J. Mrzek, F. Negoita, F. De Oliveira-Santos, Z. Podolyk, F. Pougheon, M. G. Porquet, P. Roussel-Chomaz, H. Savajols, Y. Sobolev, C. Stodel, J. Timar, and A. Yamamoto, Phys. Rev. C **69**, 034312 (2004).
[8] J. R. Terry and J. L. Lecouey, Nucl. Phys. **A734**, 469 (2004).
[9] A. T. Reed, O. Tarasov, R. D. Page, D. Guillemaud-Mueller, Yu. E. Penionzhkevich, R. G. Allatt, J. C. Anglique, R. Anne, C. Borcea, V. Burjan, W. N. Catford, Z. Dlouhy, C. Donzaud, S. Grevy, M. Lewitowicz, S. M. Lukyanov, F. M. Marques, G. Martinez, A. C. Mueller, P. J. Nolan, J. Novak, N. A. Orr, F. Pougheon, P. H. Regan, M. G. Saint-Laurent, T. Siiskonen, E. Sokol, O. Sorlin, J. Suhonen, W. Trinder, and S. M. Vincent, Phys. Rev. C **60**, 024311 (1999).
[10] K. H. Wilcox, N. A. Jelley, G. J. Wozniak, R. B. Weisenmiller, H. L. Harney, and J. Cerny, Phys. Rev. Lett. **30**, 866 (1973).
[11] C. L. Woods, L. K. Fifield, R. A. Bark, P. V. Drumm, and M. A. C. Hotchkis, Nucl. Phys. **A437**, 454 (1985).
[12] W. N. Catford, R. C. Lemmon, M. Labiche, C. N. Timis, N. A. Orr, L. Caballero, R. Chapman, M. Chartier, M. Rejmund, H. Savajols, and the TIARA Collaboration, Eur. Phys. J. A **25**, Suppl. 1, 245 (2005).
[13] J. I. Prisciandaro, A. C. Morton, and P. F. Mantica, Nucl. Instrum. Methods Phys. Res. A **505**, 140 (2003).
[14] W. F. Mueller, J. A. Church, T. Glasmacher, D. Gutknecht, G. Hackman, P. G. Hansen, Z. Hu, K. L. Miller, and P. Quirin, Nucl. Instrum. Methods Phys. Res. A **466**, 492 (2003).
[15] P. F. Mantica, A. C. Morton, B. A. Brown, A. D. Davies, T. Glasmacher, D. E. Groh, S. N. Liddick, D. J. Morrissey, W. F. Mueller, H. Schatz, A. Stolz, S. L. Tabor, M. Honma, M. Horoi, and T. Otsuka, Phys. Rev. C **67**, 014311 (2003).
[16] D. R. Goosman, D. L. Alburger, and J. C. Hardy, Phys. Rev. C **7**, 1133 (1973).
[17] P. L. Reeder, R. A. Warner, W. K. Hensley, D. J. Vieira, and J. M. Wouters, Phys. Rev. C **44**, 1435 (1991).
[18] Yu. E. Penionzhkevich, Phys. At. Nucl. **64**, 1121 (2001).
[19] B. H. Wildenthal, Prog. Part. Nucl. Phys. **11**, 5 (1984).
[20] G. Audi and A. H. Wapstra, Nucl. Phys. **A595**, 409 (1995).
[21] N. B. Gove and M. J. Martin, Nucl. Data Tables A **10**, 205 (1971).
[22] E. Sauvan, F. Carstoiu, N. A. Orr, J. S. Winfield, M. Freer, J. C. Anglique, W. N. Catford, N. M. Clarke, N. Curtis, S. Grevy, C. Le Brun, M. Lewitowicz, E. Liegard, F. M. Marques, M. MacCormick, P. Roussel-Chomaz, M.-G. Saint Laurent, and M. Shawcross, Phys. Rev. C **69**, 044603 (2004).
[23] B. A. Brown, (private communication).